

Investigating the heat transfer characteristics of supercritical HFC-125 in low temperature organic Rankine cycle

Lazova, Marija; De Paepe, Michel

In: 2nd European sCO₂ Conference 2018

This text is provided by DuEPublico, the central repository of the University Duisburg-Essen.

This version of the e-publication may differ from a potential published print or online version.

DOI: <https://doi.org/10.17185/duepublico/46097>

URN: <urn:nbn:de:hbz:464-20180827-150949-9>

Link: <https://duepublico.uni-duisburg-essen.de:443/servlets/DocumentServlet?id=46097>

License:



This work may be used under a [Creative Commons Namensnennung 4.0 International](https://creativecommons.org/licenses/by/4.0/) license.

INVESTIGATING THE HEAT TRANSFER CHARACTERISTICS OF SUPERCRITICAL HFC-125 IN LOW-TEMPERATURE ORGANIC RANKINE CYCLES

Marija Lazova*

Research fellow

Ghent, Belgium

Email: marija.lazova@ugent.be

Michel De Paepe

Professor, PhD

Ghent, Belgium

ABSTRACT

Investigating the heat transfer phenomena of fluids at supercritical pressures started in the first half of the 20th century, for either cooling or heating applications. Several fluids (water, CO₂, helium) were tested under various conditions and configurations. For instance, CO₂ was at first used as a model fluid due to its beneficial thermophysical properties and lower critical pressure and temperature (74 bar and 31°C) compared to water. Today, the supercritical CO₂ is used as working fluid in many applications. However, in the literature there is a lack of data related to heat transfer at supercritical pressures to organic fluids in large tube diameters conducted under organic Rankine cycle (ORC) conditions. Therefore, the aim of this study is experimentally to determine the heat transfer characteristics of the fluid HFC-125 in horizontal flow and inner tube diameter of 24.8 mm. The favorable thermophysical properties and the low critical pressure and temperature (36 bar and 66°C) make HFC-125 suitable working fluid for low-temperature (~100°C) transcritical ORC technology. During the measurements the pressure was in the range of 38-55 bar, the heat flux 8-30 kW/m² and the mass flow rate of the working fluid 0.2-0.3 kg/s. The test section has a counter-flow tube-in-tube configuration with a total length of 4 m. The results show that the effects of the flow acceleration during heating process have an influence to the heat transfer rate. Furthermore, the local wall temperatures vary non-linearly, which is considerably dominant in the vicinity of the critical point of HFC-125. For determining the buoyancy effect a criterion proposed in the literature was used. It was found out that at low heat flux the buoyancy effect is less dominant. In horizontal flow the impact of the buoyancy effect strongly influences the heat transfer rate and the heat transfer regime occurring at these conditions should be studied.

INTRODUCTION

Utilization of low-temperature heat from renewable energy sources and industrial waste heat is attracting a lot of attention in the last years. The organic Rankine cycle (ORC) is one of the technologies that is used for conversion of the low-temperature heat sources into useful power. Usually the low-grade heat sources are not with constant properties (temperature, pressure, mass flow rate), which is one of the obstacles for the evaporator's operation at subcritical conditions and for maximizing the power output. However, the transcritical ORC has a higher potential, because the working fluid temperature transition is above the critical point which allows a better temperature profile match with the heat source temperature glide. The transcritical ORC cycles are mostly studied for utilizing low-temperature heat sources [1-3]. However, the ORC cycle power output depends from the design and selection of proper components, choice of appropriate working fluids [4], the temperature and the stability of the heat source etc. There are several studies related to transcritical ORC's, that use CO₂ as working fluid. Chen et.al [1] did a comparative study of transcritical CO₂ and HFC-123, with respect to convert energy from low-temperature waste heat into usable work. The results show that CO₂ power cycle has slightly higher power output. Other studies [3] [5] do an experimental validation of using CO₂ as working fluid in solar (transcritical) organic Rankine cycles. Cayer et. al reported that HFC-125 and ethane are beneficial fluids that can be used in low-temperature transcritical ORC's. In several comparative studies [4-8], HFC-125 is tested with many other organic fluids including CO₂ for low-temperature (~100°C) power generation in a transcritical ORC. Due to the lower critical pressure the required pumping power is lower compared to the other fluids and HFC-125 is considered as potential medium.

HFC-125 has beneficial thermophysical properties and low critical pressure and temperature (36.2 bar and 66°C).

Furthermore, experimental studies related to heat transfer to supercritical CO₂ for solar transcritical ORC are conducted by Niu et. al [10]. The results show that when CO₂ is near the critical region it has a significant effect on the heat transfer behavior. Moreover, there are several other organic fluids that have been tested (HFC134a, R-404A, R-410A, HCFC-22) under supercritical conditions in either heating or cooling applications as well. Garimella et al. [11] performed experimental investigation regarding supercritical heat transfer to the organic fluids R-404A and R-410A in a horizontal flow and in cooling applications. In his work small diameter tubes in the range between 0.76–3.05 mm were tested. A heat transfer correlation is applicable for pressure $1.0 < p < 1.2$ was also proposed. An experimental heat transfer investigation of HFC-134a at supercritical pressure between 45–55 bar in cooling application was done by Zhao and Jiang [12]. The inner diameter of the stainless steel tube is 4.01 mm. The tests were done at different mass fluxes and a new correlation is proposed based on the measured data. Furthermore, an experimental investigation of the heat transfer characteristics of HFCF-22 and ethanol in small vertical tubes was done by Jiang et. al [13]. From the results it was concluded that the frictional pressure drop is more significant for HFC-22 than for ethanol, while the local heat transfer coefficient increases as the enthalpy increases for both fluids.

Typical for all fluids at supercritical pressure especially near the critical pressure is the strong variation of the thermophysical properties. Due to a large compressibility and density inhomogeneity the fluid induces strong convective flows within a slight temperature changes. The specific heat capacity reaches a peak at the pseudo-critical temperature T_{pc} and apart from the density the viscosity and the thermal conductivity vary significantly within a small temperature range as well. These changes are presented in Figure 1.

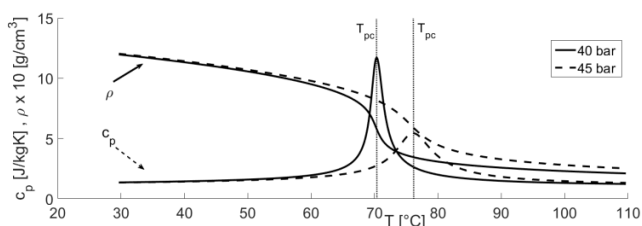


Figure 1: thermophysical property variation of HFC-125.

In order to have optimal operating ORC conditions in the heat exchanger at the hot side it is necessary to determine the behavior of the working fluid at supercritical state in horizontal flow and large tube diameter. Therefore, the main objective of this study is to determine the heat transfer characteristics of HFC-125 at supercritical pressures.

EXPERIMENTAL FACILITY “iSCORE”

An experimental facility “iSCORE” is built at the Ghent University and it consists of a heating loop, a cooling loop and an experimental loop.

A thermal oil heater Vulcanic is part of the heating loop and is depicted with a red line. The heater has a power of 20 kW and is used for providing a heating fluid (synthetic oil) to the test section.

In order to control the temperature of the cold source which is a mixture of water/glycol, a chiller with capacity of 37 kW is used. A 3-way mixing valve is installed in front of the condenser (plate heat exchanger) to control the mass flow rate of the cooling fluid. The sub-cooled working fluid HFC-125 is then provided to the circulation pump.

The experimental loop represents a transcritical organic Rankine cycle (ORC) and is depicted with a green line. This cycle consists of four basic components a pump, two heat exchangers (at the hot and cold side) and an expansion valve. The basic layout of the cycle (experimental facility) is represented in Figure 2a with a corresponding T-s diagram Figure 2b.

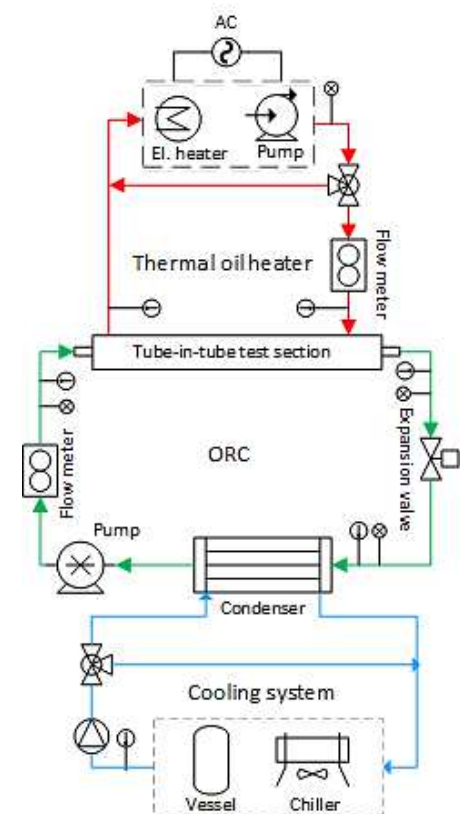


Figure 2a: layout of the experimental facility “iSCORE”.

A volumetric (positive displacement) pump (Hydra-cell, G15) is used for circulation of the working fluid HFC-125 and

is controlled by a frequency controller. The working fluid is first pressurized above its critical pressure (1-2) and heated up in the heat exchanger (test section) (2-3). The test section is positioned horizontally and is equipped with pressure and temperature sensors. In the installation there are two tube-in-tube preheaters and one in-line electrical preheater with a capacity of 10kW.

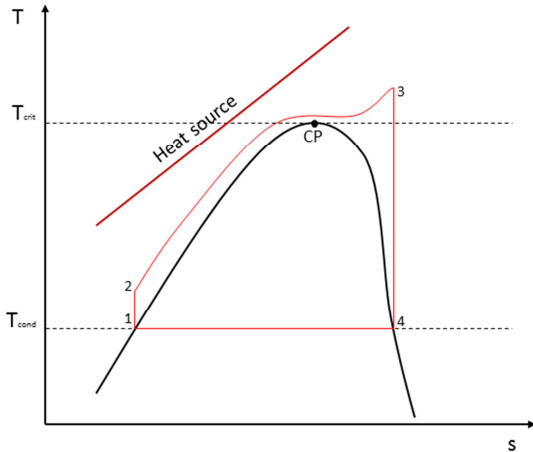


Figure 2b: temperature-entropy T-s diagram.

The tube-in-tube preheaters can be by-passed or used if there is a need. However, the inlet temperature of HFC-125 is controlled by the electrical in-line heater. An expansion valve is used to expand the working fluid (3-4). The working fluid is sub-cooled in the cooling loop (4-1) with which the cycle closes and repeats again. The process is depicted in the T-s diagram. Furthermore, Coriolis mass flow meters (GE, RHM12 and RHM20) are used to measure accurately the mass flow rate of the working and heating fluid respectively.

TEST SECTION

The test section has a configuration of a tube-in-tube heat exchanger which is positioned horizontally and is equipped with a number of sensors. A basic layout of the test section is presented on Figure 3.

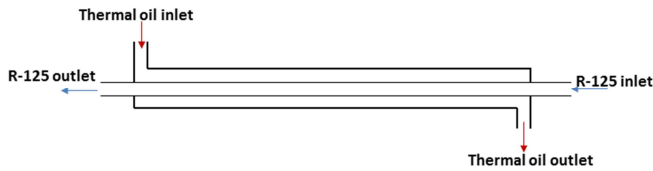


Figure 3: test section layout.

The working fluid HFC-125 circulates in the inner tube and the heating fluid (thermal oil) flows in the annulus. The inner tube is made out of a copper tube with the following dimensions: outer diameter of 28.58 mm, thickness of 1.9 mm and heating length of 4 m ($L/D_i=162$). An unheated adiabatic test section with a length of 1 m is connected to the test section

in order to provide fully-developed flow in the test section. The complete installation is insulated in order to reduce the heat losses to the environment. The temperatures at the inlet and the outlet of the test section are measured by four Pt100's. The pressure over the test section is measured by two pressure transducers. In this work, the results from the temperature and pressure measurements obtained at the inlet and outlet of the test section are reported. All signals are collected by a data acquisition system.

DETERMINING THE HEAT TRANSFER COEFFICIENT

The energy balance over the test section is determined by employing the following equations Eq. (1) and Eq. (2).

$$\dot{Q} = \dot{m}_{hf} \cdot c_p (T_{hf,in} - T_{hf,out}) \quad (1)$$

$$\dot{Q} = \dot{m}_{wf} (h_{wf,out} - h_{wf,in}) \quad (2)$$

\dot{Q} is the heat transfer rate, \dot{m}_{hf} , and \dot{m}_{wf} are the mass flow rates of the heating and working fluid respectively. The enthalpy changes of the working fluid at the inlet/outlet of the heat exchanger (test section) are given with $h_{wf,in}$ and $h_{wf,out}$. $T_{hf,in}$ and $T_{hf,out}$ are the temperature changes over the test section at the heating fluid side. The c_p is the specific heat capacity of the heating fluid.

The overall heat transfer coefficient U is determined from Eq. (3)

$$Q = U \cdot A \cdot LMTD \quad (3)$$

where A is the total surface area and $LMTD$ (logarithmic mean temperature difference) is calculated with Eq. (4)

$$LMTD = \frac{(T_{hf,in} - T_{wf,out}) - (T_{hf,out} - T_{wf,in})}{\ln \left(\frac{T_{hf,in} - T_{wf,out}}{T_{hf,out} - T_{wf,in}} \right)} \quad (4)$$

In order to determine the wall temperatures T_w , $T_{w,o}$ and $T_{w,i}$ at the outer and inner wall of the central tube the following equations were applied:

$$q = htc_o (T_{hf,b} - T_{w,o}) \quad (5)$$

$$q = htc_i (T_{w,i} - T_{wf,b}) \frac{d_i}{d_o} \quad (6)$$

$$T_w = \frac{T_{w,o} + T_{w,i}}{2} \quad (7)$$

In order to determine the Nusselt Nu number of the working fluid, Eq. (8) and (9) were used

$$\frac{1}{UA} = \frac{1}{htc_o A_o} + \frac{\ln(d_o/d_i)}{2\pi\kappa L} + \frac{1}{htc_i A_i} \quad (8)$$

$$Nu = \frac{htc_i \cdot d_{wf,hyd}}{\lambda_{wf,b}} \quad (9)$$

For calculating the annular convective heat transfer coefficient htc_o the heat transfer correlation of Dirker and Meyer [14] was used and is given with Eq. (10)

$$Nu = 0.01069Re^{0.879}Pr^{1/3} \quad (10)$$

ERROR ANALYSIS

An overview of the experimental uncertainties is presented with Table 1.

Table 1. An overview of the corresponding experimental uncertainties.

Parameter	Range	Relative error (%)
Heat input	5–10 kW	2.62
Pressure	37.5–46 bar	1.5
Temperature	45–100 °C	3.71
Mass flow rate	0.2–2.1 kg/s	2.00

However, it is important to be mentioned that the energy balance deviated less than 5% when the working fluid was away from the (super) critical region. In contrary at near and supercritical operating conditions there was a larger deviation (20%) mainly because of the enthalpy's uncertainties at this state. For determining the property changes Coolprop was used which has employed the correlations of Bell et.al [15]. Uncertainties of the Nusselt number of 9% up to 25% are found from the measurements at supercritical conditions with an average deviation of 12.7%. The mean uncertainty on the resulting overall heat transfer coefficient is 11.9%.

RESULTS AND DISCUSSION

The thermo-physical properties of the working fluid at supercritical pressures strongly depend on the changes at the bulk fluid and wall temperature. Heat transfer deterioration occurs when the bulk temperature of the working fluid is below the pseudo-critical temperature and the wall temperature significantly exceeds the pseudo-critical temperature. According to the results from the measurements, the wall temperature is higher than the bulk fluid temperature of the working fluid.

INFLUENCE OF THE WALL TEMPERATURE TO THE CONVECTIVE HEAT TRANSFER COEFFICIENTS AT VARIOUS HEAT FLUXES

The variation of the convective heat transfer coefficients HTC and the wall temperature with the global enthalpy of the working fluid at the outlet of the heat exchanger at different global heat fluxes and at mass flux of 395 kg/m²s is presented in Fig.4 (a) and (b). At lower enthalpies and lower heat fluxes (9 kW/m²; 12 kW/m²) the wall temperature variation determined from Eq's (5-7) from the measurements at the inlet and at the outlet of the test section is not very significant Fig.4 (b). However, the heat transfer coefficients at these heat fluxes are higher which shows that there is a better heat transfer between the tube wall of the heating fluid and the working fluid. At higher heat fluxes (19 kW/m²; 22 kW/m²) the enthalpy

rise yields to increased wall temperatures as well. The density and the viscosity of HFC-125 decrease at higher wall temperatures which is especially dominant near the tube wall. This results in lower heat transfer coefficients which are depicted on Fig.4 (a).

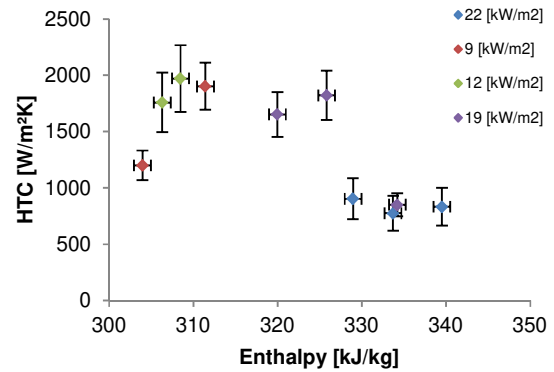


Figure 4a: heat transfer coefficients HTC variations at different heat fluxes and mass flux of 395 kg/m²s.

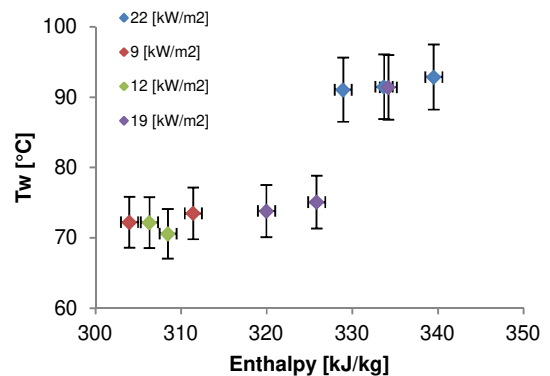


Figure 4b: wall temperatures variations at different heat fluxes and mass flux of 395 kg/m²s.

Similar effects are observed at mass fluxes in the range of 520-625 kg/m²s.

COMPARISON OF THE HEAT TRANSFER COEFFICIENTS WITH DIFFERENT HEATING FLUID TEMPERATURES AND THE RESPECTIVE BULK AND WALL TEMPERATURES

The heat transfer characteristics of a fluid at supercritical pressures differ significantly because of the thermo-physical property variation occurring at these conditions (above critical pressure and temperature). The density and viscosity changes of the fluid with the temperature have a significant influence on the heat transfer coefficients. Furthermore, Fig. 5 (a) and (b) gives an overview of the convective heat transfer coefficients HTC variations with the bulk fluid temperature T_b of HFC-125 and the wall temperature T_w . Higher heat transfer coefficients

are observed at heating fluid temperatures of 80-90°C. At these operating conditions the difference between the bulk temperature of HFC-125 and the wall temperature T_w is in the range of 8-15°C (Fig.5 (b)). At higher heating fluid temperatures of 100°C the wall temperature is higher and the temperature difference with the bulk fluid temperature is larger which can be observed on Fig. 5 (a and b). According to the results from the measurements the temperature difference is in the range of 25-35°C and these results in lower heat transfer coefficients.

However, the thermo-physical property variations of the fluid in radial direction of the tube are important which indicates that the effect of the wall temperature to the heat transfer coefficient is very significant.

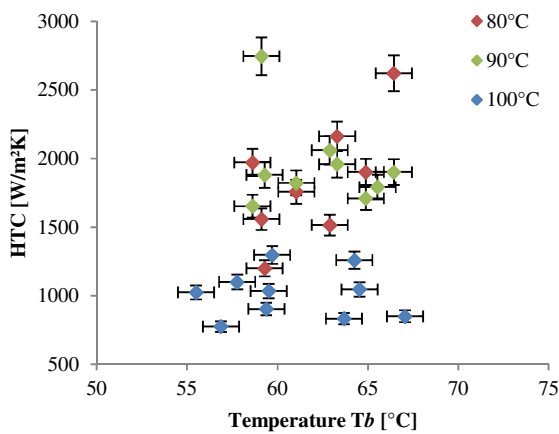


Figure 5a: evaluating the effects of the bulk temperatures to the heat transfer coefficients.

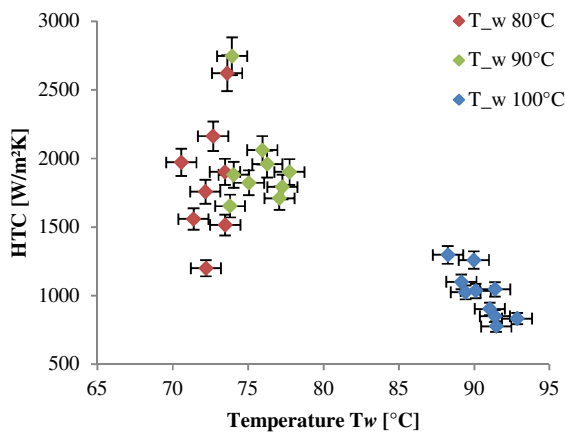


Figure 5b: evaluating the effects of the wall temperatures to the heat transfer coefficients.

DETERMINING THE EFFECTS OF THE WALL TEMPERATURE TO THE DETERIORATED HEAT TRANSFER

Determining if the effect of the heat transfer deterioration will occur at these operating conditions is of great importance. This heat transfer phenomenon (DHT) appears when there is a large increase of the tube wall temperature. An estimation of the wall heat flux at which the deteriorated heat transfer phenomena occur is presented with the Eq. (11) which is proposed by Styriakovich et al. [16]

$$q_{DHT} = 580G [W/m^2] \quad (11)$$

where q is the heat flux at which the DHT appears and G is the mass flux of the working fluid which was developed for water in Eq. (11). During the measurements the mass flux was in the range of 395-625 kg/m²s. According to results calculated with the Eq. (11) the heat flux at which DHT is expected to appear is in the range of 230-360 kW/m².

The heat flux obtained from the measurements at the temperatures of the heating fluid in the range of 80-100°C is significantly lower than the maximum heat flux determined by Eq. (11). From the calculations it can be observed that the experimental heat flux is in the range of 9-30 kW/m². This shows that a deteriorated heat transfer is not likely to occur at these operating conditions.

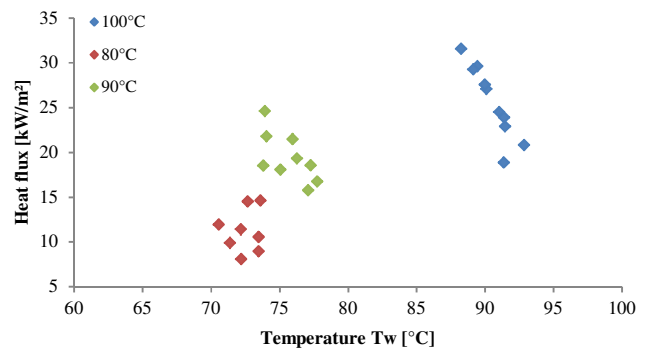


Figure 6: Determining the effects of the wall temperature to the heat flux.

However, as part of the future work is obtaining local heat transfer measurements and analyzing this phenomenon in detail for the particular working fluid and operating conditions.

CONCLUSION

In this article, preliminary results from the forced convection heat transfer measurements at supercritical state, done on the new test set-up are reported. Low-temperature heating fluid in the range of 80°C-100°C was utilized during the measurements. The presented results are all conducted by ensuring supercritical heat transfer at the working fluid side. At higher

mass flow rates the convective heat transfer coefficients reach highest values. However, at supercritical pressure and bulk fluid temperatures close to the pseudo-critical temperature there is a peak of the heat transfer coefficient. Determining the wall effects on the heat transfer mechanisms is also reported where the conclusion is that occurrence of “pseudo-critical” heat flux and hence deteriorated heat transfer is not likely to occur at these operating conditions.

A next step of this research is obtaining local heat transfer measurements and deriving a new heat transfer correlation.

NOMENCLATURE

A	total heat transfer area [m ²]
c_p	specific heat capacity [J/kg K]
d	tube diameter [mm]
D	shell diameter [mm]
f	friction factor [-]
G	mass flux [kg/m ² s]
htc	heat transfer coefficient [W/m ² K]
h	enthalpy [kJ/kg]
L	length [m]
\dot{m}	mass flow rate [kg/s]
p	pressure [bar]
T	temperature [°C]
q	heat flux [W/m ²]
Q	heat transfer rate [kW _{th}]
U	overall heat transfer coefficient [W/m ² K]

Dimensionless numbers

Nu	Nusselt number
Re	Reynolds number
Pr	Prandtl number

Greek letters

Δ	difference
λ	thermal conductivity of the fluid [W/mK]
κ	thermal conductivity of the material [W/mK]
μ	viscosity [kg/ms]
ρ	density [kg/m ³]

Subscripts

a	acceleration
ad	adiabatic
b	bulk
cr	critical
hyd	hydraulic
f	fouling
i	inner
o	outer
in	inlet conditions
out	outlet conditions
wf	working fluid
hf	heating fluid
exp	experimental
ov	overall
w	wall

ACKNOWLEDGEMENTS

The results presented in this paper have been obtained within the frame of the IWT SBO-110006 project The Next Generation Organic Rankine Cycles (www.orcnext.be), funded by the Institute for the Promotion and Innovation by Science and Technology in Flanders. This financial support is gratefully acknowledged.

REFERENCES

- [1] Y. Chen, P. Lundqvist, A. Johansson, and P. Platell, “A comparative study of the carbon dioxide transcritical power cycle compared with an organic rankine cycle with R123 as working fluid in waste heat recovery,” *Appl. Therm. Eng.*, vol. 26, no. 17–18, pp. 2142–2147, 2006.
- [2] Z. Shengjun, W. Huaixin, and G. Tao, “Performance comparison and parametric optimization of subcritical Organic Rankine Cycle (ORC) and transcritical power cycle system for low-temperature geothermal power generation,” *Appl. Energy*, vol. 88, no. 8, pp. 2740–2754, 2011.
- [3] H. Yamaguchi, X. R. Zhang, K. Fujima, M. Enomoto, and N. Sawada, “Solar energy powered Rankine cycle using supercritical CO₂,” *Appl. Therm. Eng.*, vol. 26, no. 17–18, pp. 2345–2354, 2006.
- [4] B. T. Liu, K. H. Chien, and C. C. Wang, “Effect of working fluids on organic Rankine cycle for waste heat recovery,” *Energy*, vol. 29, no. 8, pp. 1207–1217, 2004.
- [5] X. R. Zhang, H. Yamaguchi, and D. Uneno, “Experimental study on the performance of solar Rankine system using supercritical CO₂,” *Renew. Energy*, vol. 32, no. 15, pp. 2617–2628, 2007.
- [6] Z. Gu and H. Sato, “Performance of supercritical cycles for geothermal binary design,” *Energy Convers. Manag.*, vol. 43, no. 7, pp. 961–971, 2002.
- [7] Y. J. Baik, M. Kim, K. C. Chang, and S. J. Kim, “Power-based performance comparison between carbon dioxide and R125 transcritical cycles for a low-grade heat source,” *Appl. Energy*, vol. 88, no. 3, pp. 892–898, 2011.
- [8] Y. J. Baik, M. Kim, K. C. Chang, Y. S. Lee, and H. K. Yoon, “A comparative study of power optimization in low-temperature geothermal heat source driven R125 transcritical cycle and HFC organic Rankine cycles,” *Renew. Energy*, vol. 54, pp. 78–84, 2013.
- [9] G. Shu, L. Liu, H. Tian, H. Wei, and X. Xu, “Performance comparison and working fluid analysis of subcritical and transcritical dual-loop organic Rankine cycle (DORC) used in engine waste heat recovery,” *Energy Convers. Manag.*, vol. 74, pp. 35–43, 2013.
- [10] X. D. Niu, H. Yamaguchi, X. R. Zhang, Y. Iwamoto, and N. Hashitani, “Experimental study of heat transfer characteristics of supercritical CO₂ fluid in collectors of solar Rankine cycle system,” *Appl. Therm. Eng.*, vol. 31, no. 6–7, pp. 1279–1285, 2011.
- [11] S. Garimella, B. Mitra, U. C. Andresen, Y. Jiang, and B.

- M. Fronk, "Heat transfer and pressure drop during supercritical cooling of HFC refrigerant blends," *Int. J. Heat Mass Transf.*, vol. 91, pp. 477–493, 2015.
- [12] C. R. Zhao and P. X. Jiang, "Experimental study of in-tube cooling heat transfer and pressure drop characteristics of R134a at supercritical pressures," *Exp. Therm. Fluid Sci.*, vol. 35, no. 7, pp. 1293–1303, 2011.
- [13] P. X. Jiang, C. R. Zhao, and B. Liu, "Flow and heat transfer characteristics of r22 and ethanol at supercritical pressures," *J. Supercrit. Fluids*, vol. 70, pp. 75–89, 2012.
- [14] J. Dirker and J. P. Meyer, "Convective heat transfer coefficients in concentric annuli," *Heat Transf. Eng.*, vol. 26, no. 2, pp. 38–44, 2005.
- [15] I. H. Bell, J. Wronski, S. Quoilin, and V. Lemort, "Pure and pseudo-pure fluid thermophysical property evaluation and the open-source thermophysical property library coolprop," *Ind. Eng. Chem. Res.*, vol. 53, no. 6, pp. 2498–2508, 2014.
- [16] M. A. Styriakovich, T. K. Margulova, and Z. L. Miropolskiy, "Problem in the development of designs of supercritical boilers," *Teploenergetika*, vol. 14, no. 6, pp. 4–7, 1967.